Asian Journal of Chemistry Vol. 18, No. 1 (2006), 97–102

Molecular Modelling Analysis of the Interaction Between Iron(III) and L-Cysteine in Solution in Water at Low pH

FAZLUL HUQ* and MARIE C.R. PETER

School of Biomedical Sciences, Faculty of Health Sciences, C42, The University of Sydney, PO Box 170, Lidcombe, NSW 1825, Australia.

Fax: (61)(2)93519520; Tel.: (61)(2)93519522; E-mail: f.huq@fhs.usyd.edu.au

The interaction between iron(III) and L-cysteine, an amino acid, in solution in water at low pH has been investigated by UV-Visible spectrophotometry using the technique of continuous variation and molecular modelling. The absorbance value at λ_{max} was plotted against concentrations of reactants. The maximum in the absorbance *vs.* concentration graph gave the ratio at which Fe^{3+} and L-cysteine combined. At low pH, iron(III) is found to form predominantly 1 : 1 complex with L-cysteine in which iron has a distorted tetrahedral coordination geometry. In the complex, cysteine acts as a tridentate ligand being bonded to Fe(III) through amino nitrogen, carboxyl oxygen and deprotonated sulfhydryl group. The fourth position in the coordination geometry is occupied by a water molecule. The proposed structure of the complex has been optimized and its electronic spectrum generated based on molecular mechanics and semi-empirical calculations. Comparison of the observed and predicted electronic spectra of the complex indicates that iron(III) in the complex is in the high spin state with a spin multiplicity of 6.

Key Words: Amino acids, Cysteine, Iron(III), UV-visible spectra, Molecular modelling.

INTRODUCTION

Iron participates in a number of processes and biochemical reactions that are critical to the survival of all terrestrial life forms[1], including reduction of ribonucleotide (DNA synthesis), energy production (respiration), energy conversion (photosynthesis), nitrogen reduction, oxygen transport (respiration and muscle contraction) and oxygenation (*e.g.*, steroid synthesis, solubilization and detoxification of aromatic compounds). Iron is found in many different metalloenzymes including nitrogenases, oxidases, hydrogenases, reductases, dehydrogenases, deoxygenases and dehydrases. Both iron(II) and iron(III) complex with a number of donor centres including halides, cyanides, oxygen and sulfur ligands, chelating amines and porphyrins. Oxygen ligands have a high affinity for Fe^{3+} and complexes are formed with many donor ligands including

phosphates and oxalate ions, glycerol and sugars[2]. Amino acids provide excellent donor centres for both Fe^{2+} and Fe^{3+} and in iron-containing proteins both iron(II) and iron(III) are involved in covalent interactions with amino acids. Both iron(II) and iron(III) bind strongly with sulfur centres so that in many proteins and enzymes iron-sulfur clusters are found. Iron catalyzes the production of reactive oxygen species (ROS) through Fenton reaction which may be modified due to the presence of thiol compounds[3]. It has been suggested that cysteine-iron interaction may in part be responsible for the excessive toxicity of free cysteine in contrast to glutathione and N-acetyl cysteine. Reaction between iron(III) and cysteine is always preceded by complex formation[4]. Three reactive complex species: FeL^+, Fe(OH)L and $Fe(OH)L_2^{2-}$ (where L = L-cysteine) have been identified spectrophotometrically within the pH range 2.5–12.0. The blue FeL^+ is formed at low pH and is highly unstable whereas the purple $Fe(OH)L_2^{2-}$ is remarkably stable that is formed at high pH. In FeL^+, iron has a tetrahedral coordination.

In this study, the interaction between Fe^{3+} and L-cysteine (Cys) has been followed by UV-visible spectrophotometry using the technique of continuous variation and molecular modelling. Specifically, our aim has been to investigate to find out whether molecular modelling calculations provide information about the spin state of iron in the compound. Metal ion-amino acid interaction has been studied widely both in the solid state and in solution in water using a number of instrumental techniques[4–13]. But the works done on modelling the interaction between transition metal ions and amino acids in solution in water appear to be limited. In a recent paper, Rulisek *et al.*[14] report on metal ion selectivity based on DFT calculations of interaction energies of amino acid side chains with selected transition metal ions. In an earlier study, we used molecular modelling to explore the interaction between Ni^{2+} and nucleobases, nucleosides and nucleotides[15].

EXPERIMENTAL

Analytical grade iron(III) nitrate [$Fe(NO_3)_3 \cdot 6H_2O$] was purchased from Ajax Chemicals, NSW, Australia. Amino acids were purchased from Sigma-Aldrich Pvt. Ltd., NSW, Australia.

0 to 4 mL of 33.3 mM solutions of $Fe(NO_3)_3 \cdot 6H_2O$ made in 0.100 M HNO_3 and 100.0 mM Cys made in milli-Q (mQ) water, both kept at 2°C, were mixed in varying proportions and the total volume made up to 4 mL (Table-1). The UV-Visible spectrum of solution 1 (Table-1) was quickly recorded (within 40 s) using a Cary 1A UV-Visible spectrophotometer, to determine the wavelength (λ_{max}) at which the absorbance was a maximum. A scan rate of 200 nm per min and bandwidth of 2 nm were used. The absorbance at λ_{max} was then measured for each solution A to S within 40 s after mixing of the components. Milli-Q water was used as the blank. The absorbance values (Table-1) were then plotted against

the added concentrations of the amino acid to determine the stoichiometry of the adducts formed.

TABLE-1
INTERACTION BETWEEN $Fe(NO_3)_3 \cdot 6H_2O$ (33.3 mmol L^{-1}) MADE IN HNO_3 (0.100 M) AND L-CYSTEINE (100.0 mmol L^{-1}) MADE IN mQ WATER AT 2°C: ABSORBANCE VALUES AT 622 nm AGAINST mQ WATER AS THE BLANK

Solution	A	B	C	D	E	F	G	H	I
Fe^{3+} (mL)	4.00	3.75	3.50	3.25	3.00	2.75	2.50	2.25	2.00
Cys (mL)	0.00	0.25	0.50	0.75	1.00	1.25	1.50	1.75	2.00
[Fe^{3+}] (mM)	33.3	31.3	29.2	27.1	25.0	22.9	20.8	18.7	16.7
[Cys] (mM)	0	6.3	12.5	18.8	25.0	31.3	37.5	43.8	50.0
Molar ratio: n(Cys)/n(Fe^{3+})	0.000	0.200	0.429	0.692	1.000	1.364	1.800	2.333	3.000
Absorbance at 622 nm after 40 s	0.012	0.355	0.654	0.803	0.950	0.880	0.811	0.720	0.662

Solution	J	K	L	M	N	O	P	Q	R	S
Fe^{3+} (mL)	1.75	1.50	1.25	1.125	1.00	0.875	0.75	0.50	0.25	0.00
Cys (mL)	2.25	2.50	2.75	2.875	3.00	3.125	3.25	3.50	3.75	4.00
[Fe^{3+}] (mM)	14.6	12.5	10.4	9.4	8.3	7.3	6.2	4.2	2.1	0
[Cys] (mM)	56.3	62.5	68.8	71.9	75.0	78.1	81.3	87.5	93.8	100
Molar ratio: n(Cys)/n(Fe^{3+})	3.857	5.000	6.600	7.667	9.000	10.69	13.00	21.00	45.00	—
Absorbance at 622 nm after 40 s	0.612	0.552	0.457	0.426	0.378	0.359	0.331	0.254	0.155	0.007

HyperChem Calculations

The proposed structure of the Fe(III)-cysteine complex was optimized and its electronic spectrum generated based on molecular mechanics and semi-empirical calculations using HyperChem Molecular Visualization and Simulation program[16]. Geometry optimizations based on molecular mechanics (using MM^+ force field) and semi-empirical calculations (using PM3)[17] were used to find the coordinates of molecular structures that represent a potential energy minimum (ZINDO/1 calculations were not used as the calculations resulted into unrealistically distorted structure for the complex). For geometry optimization using both molecular mechanics and semi-empirical calculations, Polak-Ribiere routine with RMS gradient of 0.02 as the termination condition was used. To simulate the conditions in solution, the molecules were placed in a periodic box of TIP3P water molecules[18] followed by further cycles of geometry optimization. The actual dimensions of the box used and the maximum number of water molecules present were $18.70 \times 18.70 \times 18.70$ Å and 216, respectively. The minimum distance between solvent molecules and solute atoms was set at 2.3 Å. Molecular dynamics calculations were used to obtain a lower energy minimum by enabling molecules

to cross potential barriers[19]. The parameters used in simulated annealing were: heat time = 1 ps, run time = 0.5 ps, cool time = 0 ps, step size = 0.0005 ps, bath relaxation time = 0.1 ps, starting temperature = 100 K, simulation temperature = 300 K, temperature step = 30 K and data collection period = 4 time steps.

For the optimized structures, electronic spectra were generated using the routine ZINDO/S following a singly excited configuration interaction (CI) calculation with semi-empirical method. HyperChem performs a Self Consistent Field (SCF) calculation to obtain the reference electronic configuration associated with the ground state. Next, it generates a series of singly excited configurations, computes Hamiltonian matrix elements between them and then diagonalizes the matrix to get the spectrum of the electronic states. The number of occupied and unoccupied orbitals set in the single point CI calculations was both set equal to ten.

RESULTS AND DISCUSSION

Fe^{3+} combined with L-cysteine to form a blue complex that decomposed quickly resulting into a clear solution.

Fig. 1 gives the absorbance *vs.* concentration of cysteine plot applying to the continuously varying mixtures of $Fe(NO_3)_3 \cdot 6H_2O$ (33.3 mM) and L-cysteine (100 mM) at $\lambda = 622$ nm. The maximum in the graph indicates the formation of predominantly 1 : 1 complex between Fe^{2+} and L-cysteine.

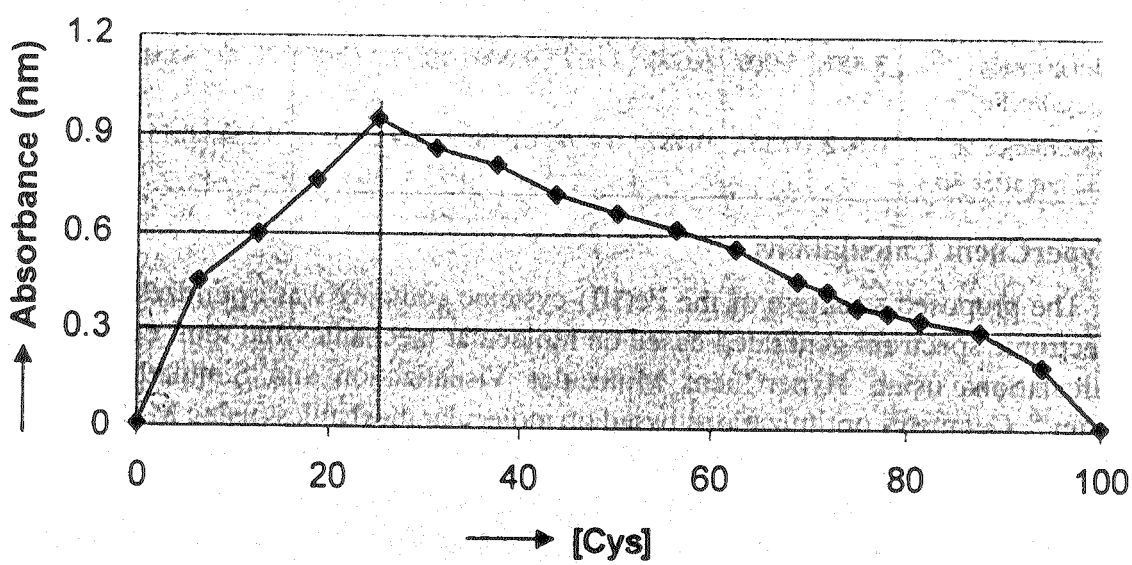

Fig. 1. Absorbance *vs.* added concentration of cysteine plot applying to the continuously varying mixtures of $Fe(NO_3)_3 \cdot 6H_2O$ (33.3 mM) made in HNO_3 (0.100 M) and L-cysteine (100 mM) made in mQ water at 2°C, indicating the formation of 1 : 1 complex between Fe^{3+} and L-cysteine

For iron(III)-L-cysteine complex, best agreement between observed and predicted electronic spectra was found when iron(III) was considered to be coordinated to the cysteine ligand (through amino nitrogen, carboxyl oxygen and

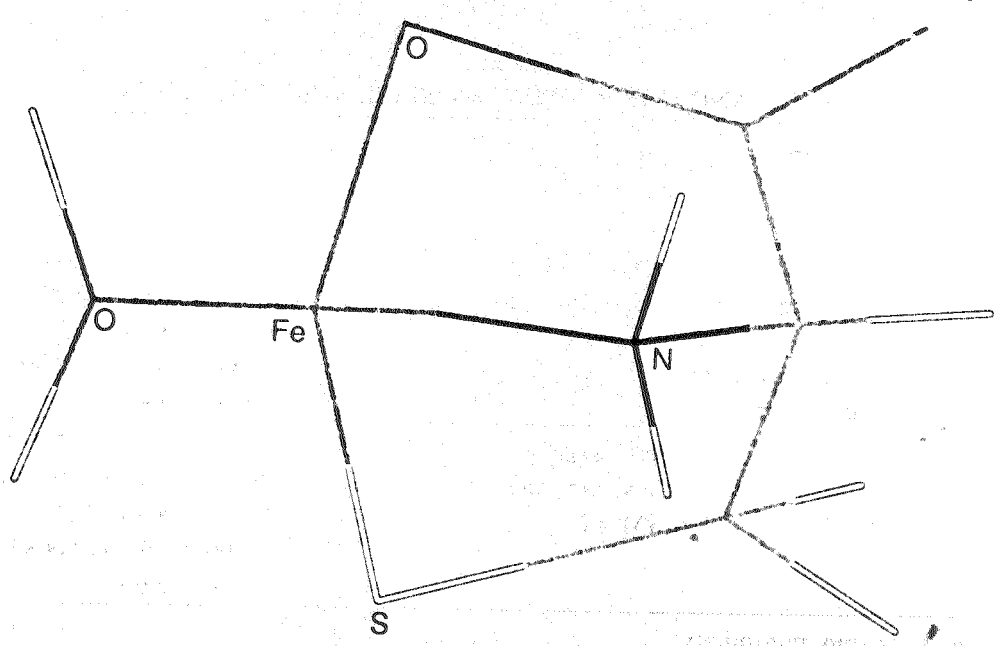

Fig. 2. Proposed structure of $Fe(Cys)(H_2O)^+$ in which Fe^{3+} is bonded to one L-cysteine ligand through amino nitrogen, carboxyl oxygen and deprotonated sulfhydryl group and one water molecule

deprotonated sulfhydryl group) and one water molecule so that the complex ion had the stoichiometry $Fe(Cys)(H_2O)^+$.

In the structure, iron(III) is considered to be in high spin state with a spin multiplicity of 6 as it gives a better agreement between observed and predicted electronic spectra than when iron(III) is considered to be in low spin state. The predicted absorption maximum in the optimized structure of $Fe(Cys)(H_2O)^+$ is found to be at 620.0 nm as compared to the observed values of 622.0 nm. When iron was considered to be in low spin state with a spin multiplicity of 2, the predicted electronic spectral maximum was 471.3 nm. It may be noted that Fe(III) is in high spin state with nearly all its complexes, except with very strong ligands such as CN^-, bipyridine and phenanthroline[2]. Thus that in the complex $Fe(Cys)(H_2O)^+$, Fe^{3+} is in the high spin state is not unexpected (Table-2).

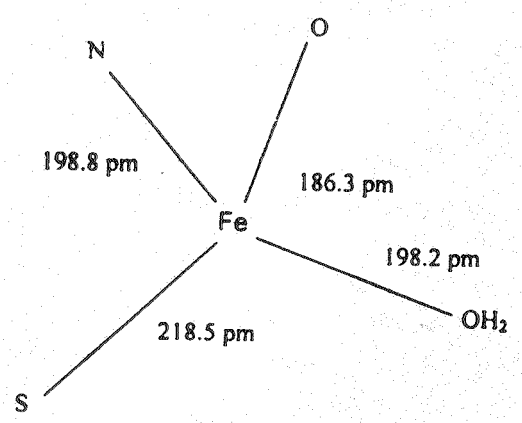

Fig. 3. Bond distances and angles illustrating distorted tetrahedral coordination geometry around Fe(III)

The bond distances and bond angles given in Fig. 3 show that the coordination geometry around iron in the optimized high spin structure is a distorted tetrahedron.

TABLE-2
OBSERVED AND COMPUTED UV-VISIBLE SPECTRAL LINES

Complex	Observed λ_{max} values (nm)	Structure/Spin state	Structure/Total energy/ΔH_f (kcal mol^{-1})	Predicted spectral lines (nm)
$Fe(Cys)(H_2O)^+$	A broad band ranging from 500 to 770 nm with maximum at 622 nm	$Fe(Cys)_4(H_2O)^+$ / High spin state (SM* = 6)	–59362.47; –7959.31	679.5 (0.0087), 620.4 (0.0164), 457.8 (0.0013), 438.8 (0.0024), 423.1 (0.0014), 415.0 (0.0086), 250.4 (0.0043)
		$Fe(Cys)_4(H_2O)^+$/ Low spin state (SM = 2)	–59497.75; –8094.60	471.3 (0.0093), 437.7 (0.0017), 381.9 (0.0334), 360.8 (0.0036), 327.5 (0.0093), 293.0 (0.0083), 261.9 (0.0069)

*SM stands for spin multiplicity

Conclusion

In solution in water at low pH, iron(III) forms blue highly unstable 1 : 1 complex with L-cysteine in which iron has a tetrahedral geometry. Molecular modeling calculations support the idea that iron(III) in the complex $Fe(Cys)(H_2O)^+$ is in high spin state.

REFERENCES

1. E.C. Theil and K.N. Raymond in I. Bertini, H.B. Gray, S.J. Lippard and J.S. Valentine (Eds.) Bioinorganic Chemistry, University Science Books, Chapter 1, p. 1 (1994).
2. F.A. Cotton, G. Wilkinson, C.A. Murillo and M. Bocham, John Wiley & Sons, Inc., New York, Chapter 17, pp. 692–876 (1999).
3. E.Y. Yang, A. Campbell and S.C. Bondy, *Redox Report*, **5**, 371 (2000).
4. R.F. Jameson and W. Linert, *Monastshefte fuer Chemie*, **122**, 887 (1991).
5. C. Sennet, L.E.G. Rosenberg and I.S. Milman, *Ann. Rev. Biochem.*, **50**, 1053 (1981).
6. In: H. Sigel (Ed.), Metal Ions in Biological Systems, Vol. 2, Marcel-Dekker, New York, Chapter 2 (1973).
7. D.S. Barnes and L.D. Pettit, *J. Inorg. Nucl. Chem.*, **33**, 2177 (1971).
8. P.J. Morris, R.B. Martin and R. Bruce, *J. Inorg. Nucl. Chem.*, **33**, 2891 (1971).
9. I. Ting Po, E.J. Burke, J.L. Meyer and G.H. Nancollas, *Thermochim. Acta*, **5**, 463 (1973).
10. R.W. Hay and D.R. Williams, *Amino-Acids, Pept. Protein*, **9**, 494 (1978).
11. W.J. Puspita, Y. Funahashi, A. Odani and O. Yamauchi, *J. Inorg. Biochem.*, **67**, 294 (1997).
12. Q.P. Lei and I.J. Amster, *J. Am. Soc. Mass Spectrom.*, **7**, 722 (1996).
13. L. Rulisek, *Chemicke Listy*, **95**, 796 (2001).
14. L. Rulisek and Z. Havlas, *J. Am. Chem. Soc.*, **122**, 10428 (2001).
15. F. Huq and M.C.R. Peter, *J. Inorg. Biochem.*, **78**, 217 (2000).
16. HyperCube HyperChem, Release 7 for Windows, 7.0 ed.; HyperCube, Ed. (2002).
17. J. Ridley and M.C. Zerner, *Theoret. Chim. Acta*, **42**, 223 (1976).
18. W.L. Jorgenson, J. Chandrasekhar, J.D. Madura, R.W. Impey and M.L. Klein, *J. Chem. Phys.*, **79**, 926 91983).
19. H.R. Macke and A.F. Williams, in: MA Fox and M. Chanon (Eds.), Photoinduced Electron Transfer, Elsevier, Amsterdam (1998).

(*Received*: 8 September, 2004; *Accepted*: 5 September 2005) AJC-4368